INFRARED THERMOGRAPHIC METHOD FOR DEPTH CHARACTERIZATION OF LOW SIZE/DEPTH ASPECT RATIO DEFECTS IN METAL PARTS

[1]Alexey Moskovchenko, [2]Michal Švantner, [3]Lukáš Muzika

[1]New technologies research center, University of West Bohemia, Plzeň, Czech Republic, EU,
alexeym@ntc.zcu.cz
[2]New technologies research center, University of West Bohemia, Plzeň, Czech Republic, EU,
msvantne@ntc.zcu.cz
[3]New technologies research center, University of West Bohemia, Plzeň, Czech Republic, EU,
muzika@ntc.zcu.cz

DOI -

Abstract

Infrared thermography is a fast and illustrative nondestructive testing method, which is widely used for an inspection of metallic and non-metallic materials. Previously it was used mostly for defects indication. However, modern devices and software allow an application of a quantitative estimation of parameters of the defects. This contribution presents a novel infrared thermographic method for quantitative defect depth estimation. The majority of known thermographic techniques is based on a 1D heat transfer model and does not take into account 3D heat transfer. These methods are applicable only for large defects, which lateral size can be assumed as infinite. In contrast, the presented technique takes into account lateral dimension of defects and a finite thickness of a tested material. The method is based on a modification of the 1D analytical solution obtained by Almond et al. and a nonlinear optimization procedure. The algorithm was verified by numerical modelling and flash-pulse thermographic inspection experiments. Applicability of the method for the defect depth evaluation in the duraluminum parts was demonstrated.

Keywords: flash pulse thermography, defect depth, thermographic inspection, depth estimation

1. INTRODUCTION

Infrared (IR) thermography is widely used nondestructive inspection method for both metallic and non-metallic materials. The popularity of the IR thermography is growing in different industrial spheres such as aerospace, civil engineering, energetics [1,2]. High productivity of the inspection, illustrative data representation and non-contact inspection make it a promising nondestructive testing method for manufacturing and exploitation of different materials [3].

Quantitative defect evaluation (determination of defect depth, lateral size, and thermal resistance) is the important procedure forwarded to the assessment of quality and lifetime of the inspected material and the necessity of repair works.

Plenty of studies have been aimed to the thermographic defect depth characterization of large enough defects (when 1D heat transfer model is applicable) [4–6]. However, the depth estimation of defects with low size/depth aspect ratio is more complicated task. 3D heat diffusion processes should be taken into account in this case. The new defect depth estimation technique, which takes into account the defect size and shape, was presented by the authors in previous study [7]. This method is based on modified analytical model obtained by Almond et al [8] and nonlinear fitting procedures [9]. The presented method demonstrated good accuracy of defect depth estimation in plastic samples. However, it was not tested on

the high conductive materials such as metals where the heat transfer process is much faster. Since this method is based on the analytical model of heating by Dirac heat pulse, the real finite pulse length affects the results and deform temperature evolution curves. This effect is more significant in high conductive materials. Another problem of this model is that it assumes a semi-infinite body. It means it is appropriate for thick materials (when the thickness of the material is significantly higher than defect depth).

This work is aimed to test the applicability of the presented method to estimate defect depth in steel components. The analytical equation was modified to take into account the depth of tested sample, that allows to estimate defect depth in thinner components.

2. THEORY

Pulse thermography is based on heating of an observed surface by a short heat pulse and observing the temperature evolution of the cooling stage. The temperature of the non-defect area follows close to an analytical solution for the semi-infinite body after a Dirac pulse [10]:

$$T(0,t) = \frac{Q_0}{\sqrt{\pi\rho Ckt}} = \frac{Q_0}{e\sqrt{\pi t}} \quad , \tag{1}$$

where $T(0,t)$ is a temperature on the surface (x=0) at a time t after a Dirac heating pulse with an energy intensity Q_0. ρ, C, k and e_m are density, specific heat capacity, thermal conductivity and thermal effusivity of the material, respectively. A region containing a delamination-like defect may be considered as a slab of thickness d. The impulse response of such a slab can be expressed as [11]:

$$T(0,t) = \frac{Q_0}{e_m\sqrt{\pi t}}\left[1 + 2\sum_{n=1}^{\infty} R^n e^{-\frac{(nL)^2}{\alpha t}}\right] \tag{2}$$

The temperature contrast $\Delta T = T_d - T_{nd}$ under the defect in semi-infinite body can be obtained by subtraction eq. 1 from eq. 2:

$$\Delta T(0,t) = \frac{2Q_0}{e\sqrt{\pi t}}\left[\sum_{n=1}^{\infty} R^n e^{-\frac{(nd)^2}{\alpha t}}\right] \tag{3}$$

Then the temperature contrast under the defect of depth d in the slab of thickness L:

$$\Delta T(0,t) = \frac{2Q_0}{e\sqrt{\pi t}}\left[\sum_{n=1}^{\infty} R^n e^{-\frac{(nd)^2}{\alpha t}} - \sum_{n=1}^{\infty} 1^n e^{-\frac{(nL)^2}{\alpha t}}\right] \tag{4}$$

R_d and R_L are thermal reflection coefficients of the defect and back surface respectively.

The simplified model of temperature contrast evolution taking into account finite defect size was developed by Almond [8]:

$$\Delta T(0,t) = \frac{2Q_0}{e\sqrt{\pi t}}\left[\sum_{n=1}^{\infty} R^n e^{-\frac{(nd)^2}{\alpha t}}\right]\left(1 - e^{-\frac{D^2}{16m\alpha t}}\right) \tag{5}$$

where D- is the diameter of the defect. It was demonstrated that the variation of thermal reflection coefficient R in eq. (5) allow to model growing front of temperature contrast under the defects of different shapes (flat bottom holes, discs and bubbles).

Combining equations (4) and (5) we suggest to model temperature contrast under the defect of diameter D and depth d in slab with thickness L by following expression:

$$\Delta T(t) = \frac{2Q_0}{e\sqrt{\pi t}}\left[\sum_{n=1}^{\infty} R^n e^{-\frac{(nd)^2}{\alpha t}} - \sum_{n=1}^{\infty} 1^n e^{-\frac{(nL)^2}{\alpha t}}\right]\left(1 - e^{-\frac{D^2}{16m\alpha t}}\right) \tag{6}$$

An optimization procedure allows finding optimal values of unknown parameters of equation (6) by fitting them to experimental data. The proposed procedure includes Matlab nonlinear fitting solver and it is represented as:

$$\min_{R,d,D,e_{app},\alpha} \left\| \Delta\overline{T}(t) - \Delta T(t) \right\|, \quad (7)$$

where $\Delta T(t) = T_d - T_{nd}$ is the experimental temperature contrast between the center of the defect and non-defect area, $\Delta\overline{T}(t)$ - analytical temperature evolution (eq. 6). This method is described in detail in [7].

3. NUMERICAL MODEL AND EXPERIMENTAL SETUP

The numerical modelling was provided to study the applicability of the analytical model to predict the temperature evolution affected by 3D heat diffusion and finite heat pulse in a high conductivity material. The modelling was performed by Comsol Multiphysics software. The numerical model represented 3D heat transfer process in a solid block with air flat bottom hole defect inside after heating of its front surface by a uniform heat flux. The depth *d* and diameter *D* of the defect and thickness *L* of the block varied from 1 to 3 mm, 1 to 10 mm and 1.2 to 10 mm respectively. The numerical model was described in detail in the work [7]. Thermal properties of the solid block were: density ρ=7800kg/m^3, thermal conductivity k=54 W/(m·K) and heat capacity Cp=465 J/(kg·K). Initial temperature was 293.15 K. Inward heat flux power density $Q_0=10^7$ W/m^2, time of heating t_h=0.007 s.

Results of the numerical modelling represented temperature evolution on the surface of the block at the center of the defect (defect temperature) and in the corner of the block (non-defect temperature).

The experimental study represented the flash-pulse thermography of the duralumin sample with artificial defects. The sample was 10 mm thick duralumin plate with 40 flat bottom hole (FBH) defects. Depth of the defects varied from 2 to 9 mm and their diameter was in the range from 2 to 10 mm. Heating was performed by a flash lamp (Hensel) with energy 6 kJ. Thermographic sequences were captured by an IR camera FLIR A6751 with framerate 100 Hz and resolution 640x512 pixels. The length of the captured sequences was 1500 frames.

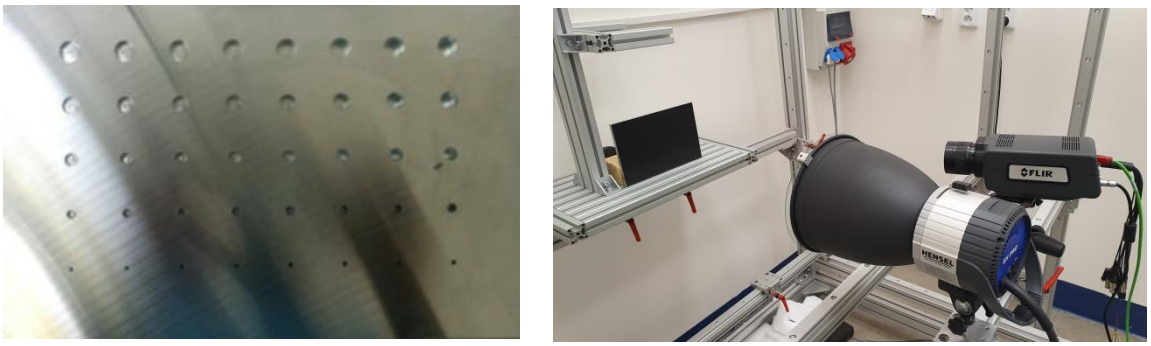

a) b)

Figure 1 The rear side of the duralumin sample (a) and experimental setup (b)

4. RESULTS AND DISCUSSION

Figure 2 presents examples of temperature contrast evolution *ΔT* obtained by numerical and analytical models. Temperature contrast *ΔT* curves (figure 2) show better fit during the growing front of *ΔT.* The divergence grows with time and defect depth. The divergence is also higher in the case of simultaneous small diameter and thickness and deep defect (figure 2 b).

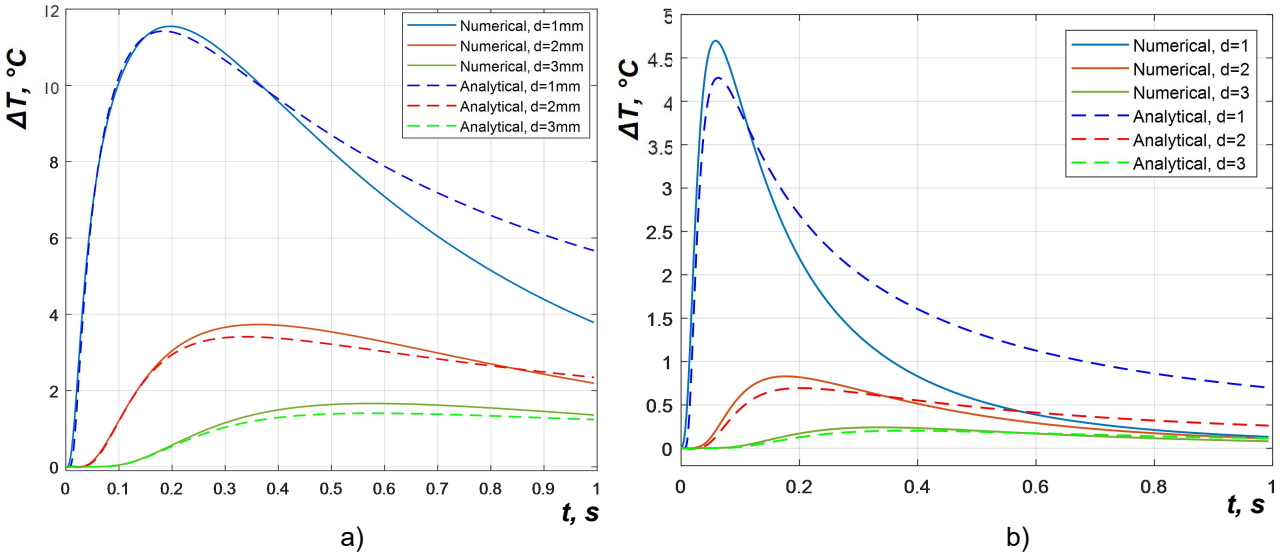

Figure 2 Numerical and analytical solution of temperature contrast evolution: a – temperature contrast ΔT (D=10, L=20), b - temperature contrast ΔT (D=3 L=5).

Despite the divergence of the analytical and numerical temperature evolution, the nonlinear fitting algorithm demonstrated good results in depth prediction. The results of the defects depth prediction by NLF algorithm are presented in table 1.

Table 1. Depth estimation by NLF algorithm applied to the numerical modelling results.

Defect depth d, mm	Defect diameter D, mm	Sample thickness L, mm	Predicted depth d_p, mm	Relative error, %
1	10	10	0.95	-5
2	10	10	1.95	-2.5
3	10	10	2.91	-3
1	3	5	0.87	-13
2	3	5	1.86	-7
3	3	5	2.80	-6,67
1	5	10	0.90	-10
1	3	10	0.88	-12
1	1	10	0.87	-13
1	5	5	0.87	-13
1	5	3	0.89	-11
1	5	1.2	0.96	-4

The relative error of the depth estimation varied from 2.5 to 13% which is a better result than other thermographic algorithms [12]. The accuracy of the depth estimation does not drop down with the increase of the depth of the defects and with the reduction of the diameter of the defects and the sample thickness. It means that the presented algorithm is applicable for the depth estimation of defects with various combinations of depth and diameter.

Figure 3 demonstrates an example of a thermogram (a) and ΔT curves as measured and fitted by the presented algorithm.

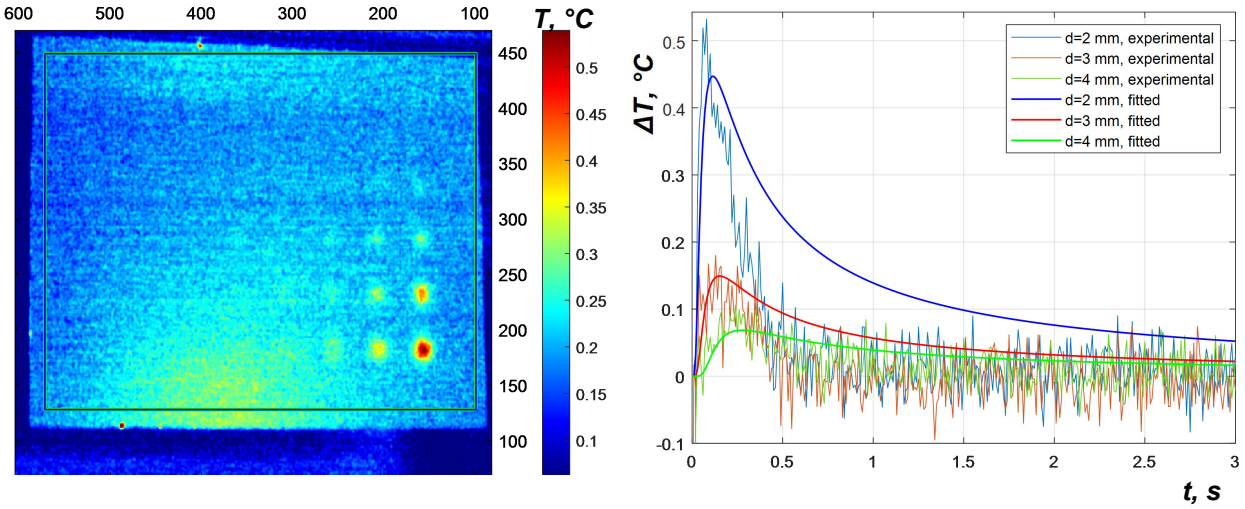

a) b)

Figure 3 Example of the IR thermogram and ΔT curves, D=10 mm

There were detected 9 defects of the depth 2-4 mm and diameter 4-10 mm in the thermogram (fig 3 a)). The experimental ΔT curves and the fitted curves obtained by NLF algorithm are presented in the figure 3 b).

Table 2 demonstrates the results of depth estimation algorithm applied to the experimental data of the thermographic testing of the duralumin sample.

Table 2. Experimental results

Defect depth *d*, mm	Defect diameter *D*, mm	Sample thickness *L*, mm	Predicted depth d_p, mm	Relative error, %
2	10	10, dural	1.94	-3
3	10	10, dural	2.41	-19.67
4	10	10, dural	3.75	-6.25
2	8	10, dural	1.61	-19.5
3	8	10, dural	2.46	-18
4	8	10, dural	3.46	-13.5
2	6	10, dural	1.45	-27.5
3	6	10, dural	1.76	-12
2	4	10, dural	1.48	-26

A relative error of experimental defect depth measurement was from 3 to 27.5%. The error may be caused by a high level of noise, weak temperature signal and fast thermal process in the high-conductive material.

5. CONCLUSION

New defect depth estimation algorithm based on nonlinear fitting and analytical model was presented in this study. In contrast to known methods, the presented algorithm takes into account finite lateral size of the defect and finite thickness of the sample. The effectivity of the algorithm was demonstrated by numerical modelling and flash-pulse thermographic inspection of duralumin sample with artificial defects. The relative error of the depth estimation was from 3 to 27.5 % in the defects depth range 2-4 mm, defects diameter range 4-10 mm and the sample thickness 10 mm. These results are promising for an application of infrared thermographic measurement of such test objects. Application of more powerful heaters and faster infrared cameras has a potential to improve accuracy of the depth estimation by this method.

ACKNOWLEDGEMENTS

This research was founded by ERDF project “LABIR-PAV/Pre-application research of infrared technologies” Reg. No. CZ.02.1.01/0.0/0.0/18_069/0010018 and by the project SGS-2022-007.

REFERENCES

[1] Parker G. Encyclopedia of Materials: Science and Technology. Guid. Opt. Commun. Mater., 2001, p. 3703–7.

[2] Kutz M. Handbook of Environmental Degradation of Materials. William Andrew; 2018.

[3] Hiasa S, Birgul R, Catbas FN. Infrared thermography for civil structural assessment: demonstrations with laboratory and field studies. J Civ Struct Heal Monit 2016;6:619–36. https://doi.org/10.1007/s13349-016-0180-9.

[4] Peeters J, Ibarra-Castanedo C, Sfarra S, Maldague X, Dirckx JJJ, Steenackers G. Robust quantitative depth estimation on CFRP samples using active thermography inspection and numerical simulation updating. NDT E Int 2017;87:119–23. https://doi.org/10.1016/j.ndteint.2017.02.003.

[5] Tang Q, Dai J, Liu J, Liu C, Liu Y, Ren C. Quantitative detection of defects based on Markov–PCA–BP algorithm using pulsed infrared thermography technology. Infrared Phys Technol 2016;77:144–8. https://doi.org/10.1016/j.infrared.2016.05.027.

[6] Vavilov VP, Burleigh DD. Review of pulsed thermal NDT: Physical principles, theory and data processing. NDT E Int 2015;73:28–52. https://doi.org/10.1016/j.ndteint.2015.03.003.

[7] Moskovchenko A, Švantner M, Vavilov V, Chulkov A. Characterizing Depth of Defects with Low Size / Depth Aspect Ratio and Low Thermal Reflection by Using Pulsed IR Thermography. Materials (Basel) 2021;14:20. https://doi.org/10.3390/ma14081886.

[8] Almond DP, Pickering SG. An analytical study of the pulsed thermography defect detection limit. J Appl Phys 2012;111:093510. https://doi.org/10.1063/1.4704684.

[9] Zhao Y, Mehnen J, Sirikham A, Roy R. A novel defect depth measurement method based on Nonlinear System Identification for pulsed thermographic inspection. Mech Syst Signal Process 2017;85:382–95. https://doi.org/10.1016/j.ymssp.2016.08.033.

[10] Carslaw HS, Jaeger JC. Conduction of heat in solids. Oxford: Oxford Univ. Press; 1959.

[11] Almond DP, Patel P, Patel PM. Photothermal Science and Techniques. Vol. 10. Springer Science & Business Media; 1996.

[12] Moskovchenko AI, Vavilov VP, Chulkov AO. Comparing the efficiency of defect depth characterization algorithms in the inspection of CFRP by using one-sided pulsed thermal NDT. Infrared Phys Technol 2020;107:103289. https://doi.org/10.1016/j.infrared.2020.103289.